First-order CO_2 trapping characteristics of fold-and-thrust belts: Assessing carbon storage potential in the Appalachian Basin and beyond

Lars W. Koehn[1], Phillip S. Prince[1], Wes Godbey[1], Mary Verne[1], Nick Fowler[1], Patrick McCrady[2], and Ryan M. Pollyea[1,3]

https://doi.org/10.1190/tle42110755.1

Abstract

Carbon capture and storage (CCS) is a strategy that is used to reduce global greenhouse gas emissions. As a result of increased government incentives and maturing carbon markets, CCS is currently experiencing an unprecedented level of public and commercial interest. In the United States, the Appalachian Basin contains abundant hydrocarbon resources and is the location of numerous industrial facilities, making the region a promising target for CCS development. However, the lack of seismic reflection surveys and well data, along with complex geologic structure throughout much of the basin, has limited the commercial interest in CCS development. This study proposes that the thin-skinned fold-and-thrust belt of the Appalachian Basin may contain geology suitable for secure long-term CO_2 storage. This region, known as the Valley and Ridge physiographic province, holds complex fold-and-thrust structures that may effectively trap commercial volumes of CO_2. We test this idea by developing a suite of kinematically feasible geologic interpretations for the Catawba syncline Pulaski thrust system in southwest Virginia. We then use these geologic models to conduct numerical simulations for CO_2 storage within the fold-and-thrust belt structures of the Catawba syncline. Our simulation results indicate that the geometric configuration of fold-and-thrust belt structures may offer commercially viable CO_2 traps for CCS projects within the Appalachian Basin and similar geologic settings worldwide.

Introduction

Carbon capture and storage (CCS) is the process of capturing CO_2 emissions from point-source industrial facilities and storing it underground in a variety of geologic reservoirs including depleted hydrocarbon fields, saline reservoirs, and mafic igneous rocks. Of these, storage in saline reservoirs has the greatest potential storage volume and the largest distribution across the United States (NETL, 2015). Similar to conventional clastic oil and gas reservoirs, saline CO_2 storage reservoirs must have sufficient porosity and permeability to hold large amounts of fluid, as well as a trap and seal system that prevents CO_2 from leaking to the surface. Furthermore, potential reservoirs should have pressure and temperatures above the critical point of CO_2 (approximately 31°C and 7.4 MPa). This allows CCS operators to transport and inject CO_2 at high density (Bachu, 2008; Benson and Cole, 2008). Commercial adoption of CCS in the oil and gas industry and other heavy-emitting industries is likely necessary to reach global emission reduction goals (IPCC, 2023).

Foreland fold-and-thrust belts are a potentially undervalued saline CCS opportunity for nearby emitting facilities. Fold-and-thrust belt deformation creates geologic structures that effectively trap hydrocarbons in many parts of the world and could potentially trap CO_2 as well. Fold-and-thrust belts are formed through compression associated with plate collision or subduction. They can be defined by the presence of a regional basal décollement and shallower thin-skinned deformation involving faulting and folding that creates stacked and/or imbricate geologic structures (Roeder, 2009; Poblet and Lisle, 2011). Fold-and-thrust belt structures (Figure 1) often have folds that act as natural reservoirs for fluids to accumulate and thrust faults that may emplace low-permeability formations that seal the underlying reservoir formation. Thrust faults may also act as barriers to flow themselves due to the presence of low-permeability fault gouge (Mitra, 1986; Mitra, 1990; Fairley and Hinds, 2004). These structures have been extensively researched and hold significant oil and gas resources across the globe including in Canada (Dahlstrom, 1970), the eastern United States (Ryder et al., 2014), Iran and the Persian Gulf (Bordenave, 2002; Bordenave and Hegre, 2010), and South America (Dunn et al., 1995; Uliana et al., 1995). The presence of significant hydrocarbon resources in fold-and-thrust belt structures indicates that the structures have high-porosity high-permeability reservoirs and effective low-permeability sealing units. Therefore, hydrocarbon-bearing fold-and-thrust belts should be considered as strong targets for commercial CCS development.

The Appalachian Basin is one such fold-and-thrust belt located in the eastern United States. The fold-and-thrust belt section of the Appalachian Basin, also known as the Valley and Ridge or Eastern Overthrust province, is defined by the area between the Blue Ridge Fault to the east (displaces crystalline rock of the Appalachian

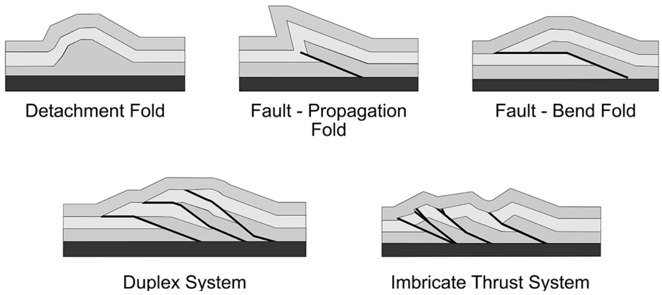

Figure 1. Examples of idealized fold-and-thrust structures that could act as structural traps for CO_2 storage. Adapted from Roeder (2009).

[1]Virginia Tech, Department of Geosciences, Blacksburg, Virginia, USA. E-mail: larskoehn99@gmail.com; psprince@vt.edu; wes20@vt.edu; vmary1@vt.edu; nlfowler4@vt.edu; rpollyea@vt.edu.
[2]Titan America LLC, Roanoke, Virginia, USA. E-mail: pmccrady@titanamerica.com.
[3]Virginia Tech, Virginia Center for Coal and Energy Research, Blacksburg, Virginia, USA.

metamorphic core) and the Alleghany Front to the west (marks the beginning of the relatively flat Appalachian Plateau). The Appalachian Basin has historically been the most productive basin for coal extraction in the United States and holds significant oil and gas reserves. The basin has produced a cumulative 34.5 billion short tons of coal and holds another 66 billion short tons in reserve (Tewalt and Ruppert, 2014). Additionally, the Appalachian Basin holds 4.76 billion barrels of oil and 124.9 trillion cubic feet of gas in ultimate recoverable oil and gas reserves (Ryder et al., 2014). This extensive hydrocarbon extraction involves numerous facilities with large CO_2 emissions that could benefit from CCS development. We note that the majority of hydrocarbon production and reserves is in the less deformed plateau section of the basin, and the majority of gas reserves exists in unconventional resources such as tight shale and coalbed methane. However, there are conventional oil and gas fields in the Valley and Ridge province that demonstrate this region's ability to hold hydrocarbon resources (e.g., Young and Harnsberger, 1955; Diecchio, 1985; Hohn et al., 1997; and Ryder and Zagroski, 2003). While research on CCS in unconventional resources such as tight shale and unmineable coal seams is ongoing, these technologies need further development to be commercially viable (Godec et al., 2014). Saline CO_2 storage, however, is a proven technology in other basins that could be implemented here. For example, the Sleipner Project, which began injecting in 1996, has successfully stored 16 million metric tons of CO_2 separated from natural gas production in Utsira sand in the North Sea (Furre et al., 2017). In the United States, the Decatur Project in the Illinois Basin stored approximately 1 million metric tons of CO_2 from ethanol fermentation between 2007 and 2014 (Greenberg et al., 2017). These two projects demonstrate the feasibility of saline storage in both onshore and offshore settings and as a carbon abatement strategy for several industries. The combination of CO_2-intensive industries and known hydrocarbon traps in the Appalachian fold-and-thrust belt may offer significant commercial opportunities for CCS development. This study will contribute to the development of commercial CCS in the Appalachian fold-and-thrust belt by assessing the CO_2-trapping characteristics of Appalachian-style fold-and-thrust structures.

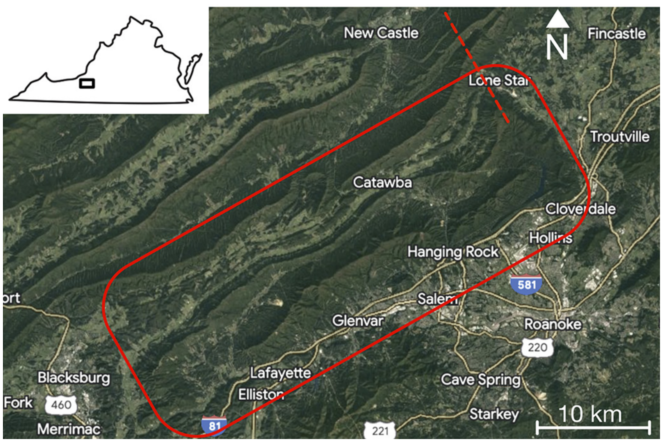

Figure 2. Approximate location of study site in southwestern Virginia (upper left). The surface expression of the Catawba syncline is indicated by the red box in the satellite image. The location of the interpreted geologic cross section (Figure 3) is indicated by the dashed line. Modified from Google Earth.

Model construction

Within the Appalachian Basin, the Catawba syncline Pulaski thrust system was selected as the study area for this project based on its proximity to local industrial emitters, the presence of a potential reservoir-seal system in the fault footwall, and its overall thin-skinned fold-and-thrust belt geology. The Catawba syncline is a doubly plunging synclinal structure in southwest Virginia that extends from Blacksburg to north of Roanoke (Figure 2). It is bounded by the Pulaski thrust system, which emplaces Cambrian-age carbonate rocks over younger Mississippian and Devonian units (Bauerlein, 1966; Broughton, 1971; Bartholomew, 1987). It is unknown if there is additional blind thrust faulting and associated structure in the Pulaski thrust sheet footwall at the western edge of the Catawba syncline. This study site is representative of the central and southern Appalachian Valley and Ridge province because it contains a large regional fold- (Catawba syncline) and-thrust system (Pulaski thrust sheet) that may be compartmentalized further by minor faults and folds (potential blind thrusting below the Pulaski thrust) developed on intermediate detachment (shale) horizons. Due to the lack of deep wells and seismic reflection surveys in the study area, three kinematically feasible cross sections were developed for the subsurface of the study area based on surface outcrop mapping (Figure 3). Scenario 1 represents geologic conditions with no deformation below the Pulaski thrust sheet, with thickening of the Devonian shale detachment horizon. Scenarios 2 and 3 feature blind thrusting and associated folding beneath the Pulaski thrust sheet, with detachment occurring in either the Ordovician Martinsburg Formation (scenario 2) or in both the Martinsburg and Cambrian Rome formations (the basal décollement of the system) (scenario 3). Scenario 1 represents the worst-case scenario in terms of CO_2 trapping because there are no geologic structures to impede the flow of CO_2 updip along the arm of the syncline. Scenarios 2 and 3 likely represent more favorable geologies because the fold-and-thrust structures impede CO_2 flow in the updip direction.

The Oriskany sandstone and Millboro shale formations were identified as potential reservoir-seal systems on the basis of known hydrocarbons in fields near our study site (e.g., Bergton gas field in Rockingham County, Virginia) (Diecchio, 1985). At Bergton, a large anticlinorium with minor folds and thrust fault structures traps natural gas in the Oriskany sandstone (Young and Harnsberger, 1955; Simmons, 1983). This site is also located in the Appalachian fold-and-thrust belt and involves faulting and folding of the same structural intervals present in the study area. Specifically, the gas play is a localized anticline developed above a blind thrust detached in the Martinsburg and is very similar to the Catawba-Pulaski geology described in scenarios 2 and 3 (Wilson and Shummaker, 1988). Therefore, it may be a useful analogue for the Pulaski thrust sheet footwall in the absence of drilling and core analysis from the Catawba-Pulaski system. Furthermore, analysis on core from Bergton Field indicates that porosity ranges from 10.9% to 12.2%, with an average permeability of 14.7 md (1.45×10^{-14} m^2). This suggests that the rock has properties that are suitable for geologic CO_2 storage (Simmons, 1983). Oriskany natural gas fields have produced volumes of gas ranging between 10 billion cubic feet and

1 trillion cubic feet, suggesting that Oriskany reservoirs are capable of holding volumes of gas that are commercially viable for CO_2 storage (Diecchio, 1985). The Midwest Regional Carbon Sequestration Partnership also conducted a carbon storage resource assessment on the Oriskany and found that the unit holds approximately 19.4 gigatons of CO_2 storage potential, but Virginia was not included in their assessment area (Wickstrom et al., 2005). Nevertheless, the assessment further supports the Oriskany as a potential carbon storage reservoir. The Millboro shale acts as a low-permeability sealing unit in gas fields near our study site, such as Bergton Field. Furthermore, stratigraphic well logs suggest that the Millboro and Needmore shales vary in thickness in the Valley and Ridge province between 175 and 430 m (Enomoto et al., 2014). The Millboro shale is therefore an effective seal based on proven low permeability and thickness, with the Needmore acting as a secondary seal. Based on these assessments, the Oriskany and Millboro formations were used as the target reservoir and primary seal, respectively, for this modeling study.

These rock properties and the three geologic scenarios were each digitized into 3D model domains, comprising 420,000 cubic grid cells with dimensions of 110 × 110 × 110 m (Figure 3, right). Each model domain is 19.3 × 5.7 km in the horizontal plane, with a maximum thickness of 4300 m below surface (835 m above mean sea level to 3465 m below mean sea level). We assigned a permeability of 14.7 md and a porosity of 12% to the model Oriskany sandstone reservoir based on core measurements from Bergton Field as discussed earlier. Permeability within sandstone reservoirs can vary by several orders of magnitude within the same formation (Tidwell and Wilson, 2000). However, due to the lack of core measurements from our study area, this project uses Bergton core values because they are likely reasonable approximations for average permeability and porosity of the Oriskany at our site. We note that these models could be improved by site-specific core measurements from the Catawba-Pulaski system. The completion interval for CO_2 injection is located at a depth of 2020–2050 m below surface, which is within the modeled Oriskany Formation and at a depth sufficient to store CO_2 in the supercritical phase. Each model scenario simulates 100 years of CO_2 injection at a constant rate of 866,000 metric tons CO_2/year, which is characteristic of CO_2 emitters throughout the region. After the 100-year injection period, the postinjection CO_2 plume migration was simulated until steady state was achieved or simulation time reached 1000 years. For this postinjection simulation, steady state is interpreted to mean that the CO_2 plume reached stabilization.

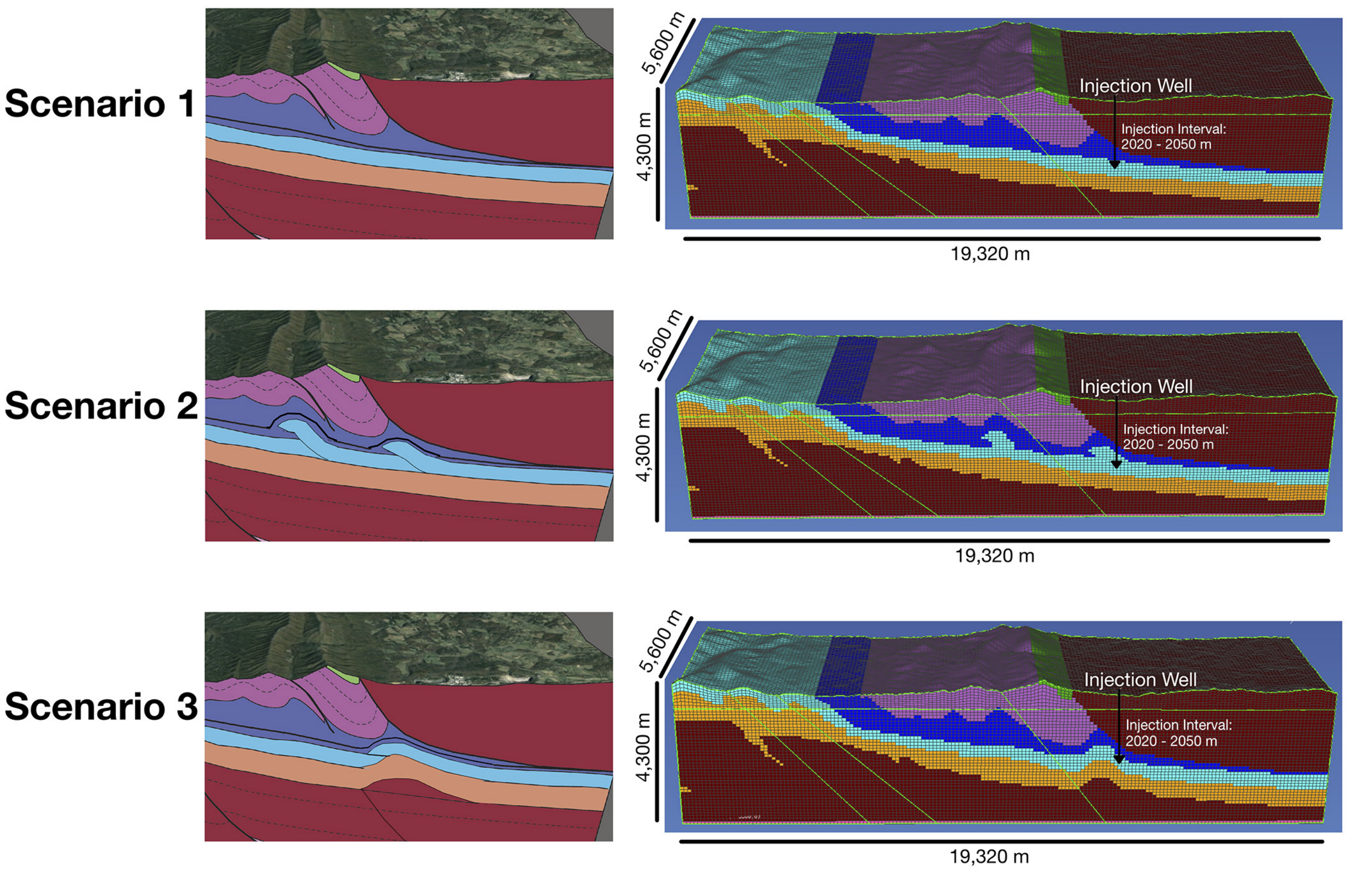

Figure 3. Three kinematically feasible cross sections (Figure 2, dashed line) for the Catawba syncline (left) and their associated cross sections through the 3D numerical model domains (right). Dark red represents Cambrian carbonate basement rocks including the Rome Formation. Orange represents Ordovician shale and limestone units including the Martinsburg Formation. Light blue represents the Lower Devonian Oriskany sandstone, which is the target reservoir of this study. Dark blue represents the Devonian Needmore and Millboro shales, which are the Pulaski thrust sheet glide horizon and the primary seals for this study. Purple represents the Upper Devonian sandstones and shale units including the Foreknobs and Brallier formations. Green represents Mississippian-age formations.

The model domains for each scenario were constructed using the graphical mesh generator in PetraSim (RockWare, 2022). In doing so, the structural cross sections for each scenario shown in Figure 3 were digitized into a Cartesian grid and extended into the out-of-plane dimension across the complete width of the model domain (5.7 km). As a result, the structural features illustrated in each cross section of Figure 3 are simulated in 3D and assumed to be relatively consistent across the out-of-plane dimension of the model domain, which is simulated as a symmetry boundary to reduce computational demand. The CO_2 injection simulation was computed for each scenario using TOUGH3 code (Jung et al., 2017) with the ECO2N v2.0 module (Pruess and Spycher, 2007; Pan et al., 2017) for nonisothermal multiphase flow of water, CO_2, and NaCl. The TOUGH3 code utilizes an integral finite-volume method in space and a first-order finite-difference method in time to solve the mass and energy conservation equations. Phase partitioning was based on local thermodynamic equilibrium. Initial pressure and temperature gradients were calculated on the basis of surface measurements and literature values (Blackwell et al., 2011). These calculations result in an average pressure gradient of 1.01×10^{-2} MPa/m (0.45 psi/ft) and an average temperature gradient of 0.018°C/m. The initial brine concentration is assumed to be 30,000 ppm. Additionally, our models incorporate van Genuchten relative permeability and capillary pressure models to compute the multiphase effects of supercritical CO_2 and brine occupying the same pore space (van Genuchten, 1980). Ideally, experimentally determined relative permeability and capillary properties for the target reservoir would be used in the model. However, we are not aware of any published CO_2 relative permeability measurements for the Oriskany sandstone, so this study makes use of literature values for a sandstone reservoir (Jung et al., 2017). Constant pressure and temperature boundaries are set on the top and lateral extent of the model domain to maintain constant fluid pressure at the surface, far-field pressure, and temperature gradients. A basal boundary heat flux of 50 mW/m^2 was applied to the model to account for the influx of geothermal heat (Blackwell et al., 2011).

Results and discussion

Simulation results suggest that the geometric configurations of fold-and-thrust structures beneath the western edge of the Catawba syncline may be suitable for CCS in all three structural scenarios illustrated in Figure 3. Under these model conditions, injected CO_2 migrates updip due to buoyancy, but the free-phase partition remains supercritical after 100 years of injection, with a phase partition comprising 84% free-phase CO_2 and 16% aqueous-phase CO_2 for all three model scenarios (Figure 4). Simulating postinjection plume migration shows that the CO_2 plume reaches stabilization (defined as a steady state) after an additional 684 years for scenario 1, 346 years for scenario 2, and 900 years for scenario 3 (Figure 5). Moreover, the anticlinal structural elements in scenarios 2 and 3 offer compelling CO_2 storage targets, even in the presence of spillover, which is discussed later in more detail. In aggregate, these results suggest that first-order structural features within thin-skinned deformation belts may be suitable CO_2 storage sinks for moderate-scale (approximately less than 1 million metric tonnes/year) industrial CO_2 emitters. While these results are generally favorable, the nature of CO_2 plume propagation and phase partitioning at stabilization varied significantly based on geologic scenario. The remainder of this section discusses simulation results for each scenario and the broader implications of map-scale structure on CO_2 storage within thin-skinned fold-and-thrust belts.

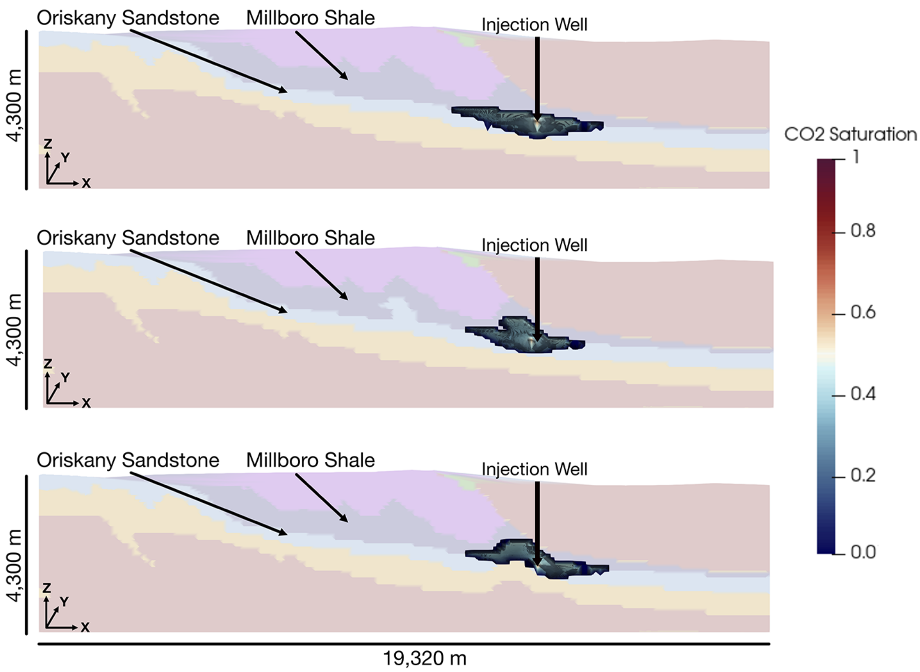

Figure 4. Simulation results of CO_2 saturation after 100 years of CO_2 injection. In all scenarios, injected CO_2 remains in the target Oriskany Formation and extends radially from the injection well. Scenario 1 features farther updip plume migration than scenarios 2 and 3 due to the lack of structural straps in scenario 1 geology.

Scenario 1. In the absence of a map-scale geologic structure, CO_2 migrates away from the well, primarily in the updip direction. After 100 years of injection, the CO_2 plume reached a maximum length in the updip direction of 3705 m (Figure 4) and a length of 2095 m in the out-of-plane direction. Hereafter, the updip direction will be denoted as the *x*-direction, and the out-of-plane direction will be denoted as the *y*-direction. During the postinjection period, the CO_2 plume continued to migrate updip, reaching an *x*-direction length of 7960 m (Figure 5) and a *y*-direction length of 2176 m. Plume stabilization was achieved 684 years postinjection when the free-phase CO_2 plume stopped migrating because buoyancy-driven CO_2 flow no longer had sufficient pressure to overcome the capillary force of the in-situ pore fluid. This is frequently referred to as capillary or residual trapping. At stabilization, the minimum depth of the free-phase CO_2 plume remained 1230 m below surface, which is still sufficient pressure and temperature conditions to keep the CO_2 in supercritical phase. In addition, the CO_2 phase partition at stabilization included 57% supercritical CO_2 ($scCO_2$) and 43% aqueous-phase CO_2 ($aqCO_2$). These results suggest that, in the absence of structural relief, CO_2 trapping within dipping beds is highly dependent on a combination of solubility trapping and hydrodynamic trapping from capillary barrier effects. In this context, the depth of injection and angle of dipping beds are fundamental considerations for CO_2 storage in the absence of structural traps. While this scenario is technically successful in storing injected CO_2, we note that the large lateral diameter of the CO_2 plume would result in a large area of review for a commercial storage project, presenting difficulties in terms of land-access agreements as well as monitoring and verification. Furthermore, updip migration of the CO_2 plume may increase the risk of contaminating drinking water resources, which are in the area at depths up to 120 m (Swain et al., 2004). While there is little risk of groundwater contamination in the simulations conducted for this study, the presence of unmapped faults or fractures could allow CO_2 and brine to leak into drinking water. These risks can be mitigated by careful site characterization prior to injection and by postinjection monitoring, including repeat seismic surveys to map the extent of the CO_2 plume and groundwater quality measurements to ensure that no leakage is occurring.

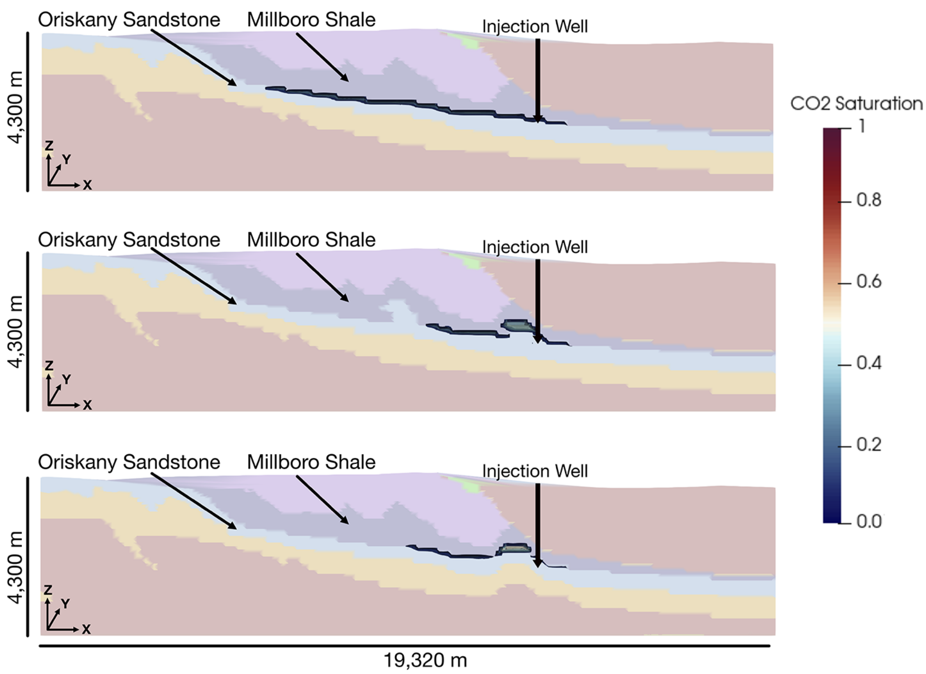

Figure 5. Free-phase CO_2 plume at plume stabilization, which is 684 years postinjection for scenario 1, 346 years postinjection for scenario 2, and 900 years postinjection for scenario 3. Note that the fold-and-thrust structures in scenarios 2 and 3 significantly impede the updip migration of the CO_2 plume in the postinjection phase.

Scenarios 2 and 3. Simulation results show that the presence of map-scale folds traps a large percentage of the injected CO_2 and limits updip migration of the plume for scenarios 2 and 3. After 100 years of injection, the CO_2 plume in scenario 2 has a length of 3160 m in the *x*-direction (Figure 4) and 2295 m in the *y*-direction. The CO_2 plume in scenario 3 has a length of 3465 m in the *x*-direction (Figure 4) and 2435 m in the *y*-direction. In comparison to scenario 1, the compact nature of these CO_2 plume dimensions offers favorable characteristics for land-access agreements, area-of-review considerations, and reduced groundwater contamination risks.

Plume stabilization for scenario 2 occurred 346 years postinjection. At stabilization, the CO_2 plume in scenario 2 has a length of 3790 m in the *x*-direction (Figure 5) and 4515 m in the *y*-direction, and the phase partition comprises 71% $scCO_2$ and 29% $aqCO_2$. For scenario 3, plume stabilization occurred approximately 900 years postinjection. At stabilization, the CO_2 plume for scenario 3 is 4240 m long in the *x*-direction (Figure 5) and 5420 m long in the *y*-direction, with a phase partition of 66% $scCO_2$ and 34% $aqCO_2$. In comparison to scenario 1, the phase partitions at stabilization for scenarios 2 and 3 comprise substantially greater free-phase CO_2. This occurs because the folds present in scenarios 2 and 3 compartmentalize CO_2 in structural highs, thus preventing CO_2 from mixing with and dissolving into formation fluids. As a result, structural compartmentalization of CO_2 minimizes the effects of solubility trapping. This means that CO_2 storage in folds will be highly dependent on the integrity of structural traps.

Although the folds are shown here to be effective structural traps, spillover of CO_2 out of the trap occurs in both scenarios, causing updip CO_2 migration. This spillover segment of the CO_2 plume fully disconnects from the portion of the plume that becomes trapped in the structural high (Figure 5) and flows updip before stabilizing when the buoyancy force equilibrates with the capillary force. As this spillover segment of the CO_2 plume migrates updip, it mixes with formation brine. This allows a larger proportion of the CO_2 to dissolve than the plume segment that remains in the fold. As a result, solubility trapping aids plume stabilization, even when spillover occurs on the updip side of the structural trap. Because plume stabilization occurs even in the presence of spillover, these results suggest that small to moderate spillover from fold traps may not be detrimental to successful CO_2 storage in fold-and-thrust belts. We further note that the presence of duplex or imbricate fold-and-thrust structures (Figure 1) offers redundancy against CO_2 spillover from a single fold trap when/if stabilization does not occur. For example, scenario 2 is a duplex fold-and-thrust system that includes a backup fold trap that would likely inhibit further updip CO_2 migration if either plume stabilization does not occur or a larger CO_2 mass is injected into the target fold.

To close this discussion about simulation results, we note that the geologic models developed here assume constant geology in the *y*-direction (beneath and outboard of the Catawba syncline).

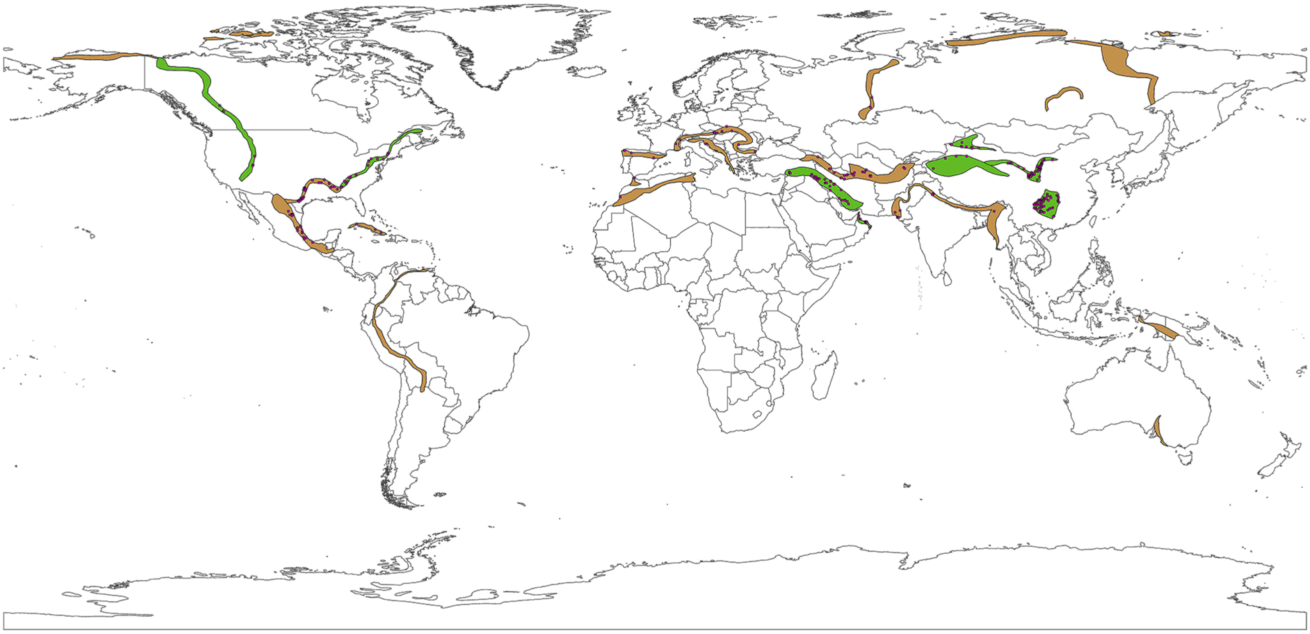

Figure 6. Map of global distribution of fold-and-thrust belts in comparison to CO_2 emissions sources in excess of 1 million metric tons per year. Map adapted from Goffey et al. (2010). CO_2 emissions data from EDGAR (2022). Pink dots denote emissions sources greater than 1 million metric tons per year. Green denotes fold-and-thrust basins that exist in close proximity to industrial sources and are considered high-value targets for CO_2 storage feasibility assessment. Yellow denotes other major fold-and-thrust belts.

However, it is possible that minor faults or folds exist below the western margin of the syncline that may further compartmentalize the area into discrete sections, significantly altering CO_2 flow patterns. These results emphasize that detailed subsurface characterization is necessary to accurately predict CO_2 storage behavior, especially in complex geologic settings such as a fold-and-thrust belts. Nevertheless, results from this study suggest that first-order trapping characteristics of fold-and-thrust belts may offer favorable trapping characteristics for commercial CO_2 storage. Specifically, we show that three kinematically feasible geologic interpretations for the Catawba syncline Pulaski thrust system in southwest Virginia are able to safely store commercial volumes of CO_2 under modeled geologic conditions. The simulation included an injection of 86.2 million metric tons of CO_2 injected over 100 years followed by postinjection simulation to achieve CO_2 plume stabilization (defined as steady state). In all geologic scenarios, the subsurface geology prevented leakage to the surface. However, the fold-and-thrust belt structures in scenarios 2 and 3 limited CO_2 plume migration by kilometers compared to scenario 1, significantly reducing leakage risk and potentially benefiting monitoring and verification efforts.

Implications for CO_2 storage in fold-and-thrust belts worldwide. Considering these simulation results in the context of matching CO_2 sources with potential CO_2 storage plays, Figure 6 illustrates the global distribution of fold-and-thrust belts that are characterized by structural features illustrated in Figure 1. Globally, industrial CO_2 emissions within fold-and-thrust belts exceed 1 billion metric tons per year (EDGAR, 2022). In this context, we ranked several fold-and-thrust belts as high-value targets for CCS because they have proven hydrocarbon resources and are near high-rate CO_2-emitting industrial facilities. Specifically, the modeling results discussed earlier may be directly relevant to the feasibility of CO_2 storage in the Appalachian Basin in the eastern United States; Canadian Rockies in western Canada; Sevier Rockies in the western United States; Zagros Belt in Iran, Iraq, Turkey, and Persian Gulf; Sub-Andes Belt in South America; Circum-Sichuan Belt in southern China; Tarim Basin belts in western China; and Yan Shan fold-and-thrust belts in northern China. In these regions, the combination of CO_2 emissions sources and potential CO_2 sinks makes these locations promising targets for commercial CCS development in geologic settings that are characterized by fold-and-thrust structural geology.

Conclusions

These results suggest that fold-and-thrust belt structures, such as the blind thrusting and associated folding in scenarios 2 and 3, create suitable traps for limiting CO_2 plume migration. However, it is clear that CO_2 trapping in these environments will require careful volumetric analysis for durable CO_2 storage. For the United States to reach its goal of net-zero CO_2 emissions, it is necessary to implement CCS in the Appalachian Basin. However, the complex structure and lack of subsurface exploration present notable challenges for CCS development. Our results support the feasibility of CCS in the Catawba syncline, while also highlighting the potential for CO_2 trapping in fold-and-thrust belt-style structural architecture. For this modeling study, we find the following.

1) Fold-and-thrust belt structures may effectively trap commercial volumes of CO_2, reduce plume propagation by kilometers, and potentially benefit commercial projects by reducing leakage risk and decreasing the area of review.

2) To the first order, CO_2 trapped within folds is highly dependent on structural trapping because solubility trapping is minimized as CO_2 displaces formation fluid in structural highs and the remaining formation fluid becomes saturated with respect to CO_2. In contrast, solubility trapping plays a fundamental role in CO_2 plume stabilization when spillover occurs on the updip limb of a fold.
3) In the absence of folds, CO_2 plume stabilization can occur by a combination of hydrodynamic capillary (or residual) trapping and solubility trapping if (1) the injection is deep and (2) the bedding dip angle is lean. However, additional research is needed to understand the parametric relationships between injection depth, capillary trapping, and dip angle.
4) Global CO_2 emissions from industrial sources exceeds 1 billion metric tons of CO_2 per year within geographic regions characterized by fold-and-thrust geology. This source-sink mapping suggests that CCS is a promising pathway for industrial-scale carbon management that should be further explored on a global scale. TLE

Acknowledgments

This material is based on work supported by the Department of Energy under award number DE-FE0031830 through the Southeast Regional Carbon Sequestration Partnership, which is managed by the Southern States Energy Board under contract number SSEB-SECARBUSA-931-VAT-2020. This manuscript was prepared as an account of work sponsored by an agency of the U.S. government. Neither the U.S. government nor any agency thereof, nor any of their employees, makes any warranty, express or implied, or assumes any legal liability or responsibility for the accuracy, completeness, or usefulness of any information, apparatus, product, or process disclosed, or represents that its use would not infringe privately owned rights. Reference herein to any specific commercial product, process, or service by trade name, trademark, manufacturer, or otherwise does not necessarily constitute or imply its endorsement, recommendation, or favoring by the U.S. government or any agency thereof. The views and opinions of authors expressed herein do not necessarily state or reflect those of the U.S. government or any agency thereof.

Data and materials availability

Data associated with this research are available and can be obtained by contacting the corresponding author.

Corresponding author: larsk@vt.edu

References

Bachu, S., 2008, CO_2 storage in geological media: Role, means, status and barriers to deployment: Progress in Energy and Combustion Science, **34**, no. 2, 254–273, https://doi.org/10.1016/j.pecs.2007.10.001.

Bartholomew, M. J., 1987, Structural evolution of the Pulaski thrust system, southwestern Virginia: GSA Bulletin, **99**, no. 4, 491–510, https://doi.org/10.1130/0016-7606(1987)99<491:SEOTPT>2.0.CO;2.

Bauerlein, H. J., 1966, Geology of the Millers Cove area, Roanoke, Craig and Montgomery counties, Virginia: M.S. thesis, Virginia Tech.

Benson, S. M., and D. R. Cole, 2008, CO_2 sequestration in deep sedimentary formations: Elements, **4**, no. 5, 325–331.

Blackwell, D., M. Richards, Z. Frone, J. Batir, A. Ruzo, R. Dingwall, and M. Williams, 2011, Temperature-at-depth maps for the conterminous U.S. and geothermal resource estimates: GRC Transactions, **35**, 1545–1550.

Bordenave, M. L., 2002, The Middle Cretaceous to Early Miocene petroleum system in the Zagros Domain of Iran, and its prospect evaluation: Presented at the Annual Convention and Exhibition, AAPG.

Bordenave, M. L., and J. A. Hegre, 2010, Current distribution of oil and gas fields in the Zagros fold belt of Iran and contiguous offshore as the result of the petroleum systems, *in* P. Leturmy and C. Robin, eds., Tectonic and stratigraphic evolution of Zagros and Makran during the Mesozoic–Cenozoic: Geological Society of London, Special Publications, 291–353, https://doi.org/10.1144/SP330.14.

Broughton, P. L., 1971, Structural geology of the Pulaski-Salem thrust sheet and the eastern end of the Christiansburg window, southwestern Virginia: M.S. thesis, Virginia Tech.

Dahlstrom, C. D. A., 1970, Structural geology of the eastern margin of the Canadian Rocky Mountains: Bulletin of Canadian Petroleum Geology, **18**, no. 3, 332–406.

Diecchio, R. J., 1985, Regional controls of gas accumulation in Oriskany sandstone, central Appalachian Basin: AAPG Bulletin, **69**, 722–732, https://doi.org/10.1306/AD4627F4-16F7-11D7-8645000102C1865D.

Dunn, F. J., K. G. Hartshorn, and P. W. Hartshorn, 1995, Structural styles and hydrocarbon potential of the Sub-Andean thrust belt of southern Bolivia, *in* A. J. Tankard, R. Soruco, and H. J. Welsink, eds., Petroleum basins of South America: AAPG.

EDGAR, 2022, Global greenhouse gas emissions, https://edgar.jrc.ec.europa.eu/dataset_ghg70, accessed 16 July 2023.

Enomoto, C. B., R. A. Olea, and J. L. Coleman Jr., 2014, Characterization of the Marcellus shale based on computer-assisted correlation of wireline logs in Virginia and West Virginia: USGS, Scientific Investigations Report 2013-5131, https://doi.org/10.3133/sir20135131.

Fairley, J. P., and J. J. Hinds, 2004, Field observation of fluid circulation patterns in a normal fault system: Geophysical Research Letters, **31**, no. 19, https://doi.org/10.1029/2004GL020812.

Furre, A-K., O. Eiken, H. Alnes, J. N. Vevatne, and A. F. Kiær, 2017, 20 years of monitoring CO_2 injection at Sleipner: Energy Procedia, **114**, 3916–3926, https://doi.org/10.1016/j.egypro.2017.03.1523.

Godec, M., G. Koperna, and J. Gale, 2014, CO_2-ECBM: A review of its status and global potential: Energy Procedia, **63**, 5858–5869, https://doi.org/10.1016/j.egypro.2014.11.619.

Goffey, G. P., J. Craig, T. Needham, and R. Scott, 2010, Fold-thrust belts: Overlooked provinces of justifiably avoided?, *in* G. P. Goffey, J. Craig, T. Needham, and R. Scott, eds., Hydrocarbons in contractional belts: Geological Society of London, Special Publications, https://doi.org/10.1144/SP348.1.

Greenberg, S. E., R. Bauer, R. Will, R. Locke II, M. Carney, H. Leetaru, and J. Medler, 2017, Geologic carbon storage at a one million tonne demonstration project: Lessons learned from the Illinois Basin — Decatur Project: Energy Procedia, **114**, 5529–5539, https://doi.org/10.1016/j.egypro.2017.03.1913.

Hohn, M. E., R. R. McDowell, D. L. Matchen, and A. G. Vargo, 1997, Heterogeneity of fluvial-deltaic reservoirs in the Appalachian Basin: A case study from a Lower Mississippian oil field in central West Virginia: AAPG Bulletin, **81**, 918–936, https://doi.org/10.1306/522B4997-1727-11D7-8645000102C1865D.

IPCC, 2023, Climate change 2022 — Impacts, adaptation and vulnerability: Cambridge University Press, https://doi.org/10.1017/9781009325844.

Jung, Y., G. S. H. Pau, S. Finsterle, and R. M. Pollyea, 2017, TOUGH3: A new efficient version of the TOUGH suite of multiphase flow and transport simulators: Computers & Geosciences, **108**, 2–7, https://doi.org/10.1016/j.cageo.2016.09.009.

Mitra, S., 1986, Duplex structures and imbricate thrust systems: Geometry, structural position, and hydrocarbon potential: AAPG Bulletin, **70**, 1087–1112, https://doi.org/10.1306/94886A7E-1704-11D7-8645000102C1865D.

Mitra S., 1990, Fault-propagation folds: Geometry, kinematic evolution, and hydrocarbon traps: AAPG Bulletin, **74**, no. 6, 921–945, https://doi.org/10.1306/0C9B23CB-1710-11D7-8645000102C1865D.

NETL, 2015, Carbon storage atlas, fifth edition: National Energy Technology Laboratory.

Pan, L., N. Spycher, C. Doughty, and K. Pruess, 2017, ECO2N V2.0: A TOUGH2 fluid property module for modeling CO_2-H_2O-NaCl systems to elevated temperatures of up to 300°C: Greenhouse Gases: Science and Technology, **7**, no. 2, 313–327, https://doi.org/10.1002/ghg.1617.

Poblet, J., and R. J. Lisle, 2011, Kinematic evolution and structural styles of fold-and-thrust belts: Geological Society of London, Special Publications, **349**, 1–24.

Pruess, K., and N. Spycher, 2007, ECO2N V2.0: A TOUGH2 fluid property module for modeling CO_2-H_2O-NACL systems to elevated temperatures of up to 300°C: Energy Conversion and Management, **48**, 1761–1767.

RockWare, 2022, PetraSim user manual, https://www.rockware.com/product/petrasim/, accessed 25 September 2023.

Roeder, D., 2009, American and Tethyan fold-thrust belts: Gebrüder Borntraeger Verlag.

Ryder, R. T., R. C. Milici, C. S. Swezey, and M. H. Trippi, 2014, Appalachian Basin oil and natural gas: Stratigraphic framework, total petroleum systems, and estimated ultimate recovery, *in* L. F. Ruppert and R. T. Ryder, eds., Coal and petroleum resources in the Appalachian Basin: Distribution, geologic framework, and geochemical character: USGS, https://doi.org/10.3133/pp1708C.1.

Ryder, R., and W. A. Zagorski, 2003, Nature, origin, and production characteristics of the Lower Silurian regional oil and gas accumulation, central Appalachian Basin, United States: AAPG Bulletin, **87**, no. 5, 847–872.

Simmons, N. G., 1983, Structural analysis of the Valley and Ridge extension of the Parsons lineament: M.S. thesis, Virginia Tech.

Swain, L. A., T. O. Mesko, and E. F. Hollyday, 2004, Summary of the hydrogeology of the Valley and Ridge, Blue Ridge, and Piedmont physiographic provinces in the eastern United States: USGS, Professional Paper 1422-A.

Tewalt, S. J., and L. F. Ruppert, 2014, Coal assessments and coal research in the Appalachian Basin, *in* L. F. Ruppert and R. T, Ryder, eds., Coal and petroleum resources in the Appalachian Basin: Distribution, geologic framework, and geochemical character: USGS.

Tidwell, V. C., and J. L. Wilson, 2000, Heterogeneity, permeability patterns, and permeability upscaling: Physical characterization of a block of Massillon sandstone exhibiting nested scales of heterogeneity: SPE Reservoir Evaluation and Engineering, **3**, 283–291, https://doi.org/10.2118/65282-PA.

Uliana, M. A., M. E. Arteaga, L. Legarreta, J. J. Cerdán, and G. O. Peroni, 1995, Inversion structures and hydrocarbon occurrence in Argentina: Geological Society of London, Special Publications, **88**, 211–233, https://doi.org/10.1144/GSL.SP.1995.088.01.13.

van Genuchten, M. T., 1980, A closed-form equation for predicting the hydraulic conductivity of unsaturated soils: Soil Science Society of America Journal, **44**, no. 5, 892–898, https://doi.org/10.2136/sssaj1980.03615995004400050002x.

Wickstrom, L. H., E. R. Venteris, J. A. Harper, J. McDonald, E. R. Slucher, K. M. Carter, S. F. Greb, et al., 2005, Characterization of geologic sequestration opportunities in the MRCSP region: Phase I task report: Midwest Regional Carbon Sequestration Partnership.

Wilson, T. H., and R. C. Shummaker, 1988, Three-dimensional structural interrelationships within Cambrian-Ordovician lithotectonic unit of central Appalachians: AAPG Bulletin, **72**, no. 5, 600–614, https://doi.org/10.1306/703C8ED9-1707-11D7-8645000102C1865D.

Young, R. S., and W. T. Harnsberger, 1955, Geology of Bergton gas field, Rockingham County, Virginia: AAPG Bulletin, **39**, no. 3, 317–328, https://doi.org/10.1306/5CEAE14B-16BB-11D7-8645000102C1865D.